

Received 21 February 2024, accepted 28 February 2024, date of publication 14 March 2024, date of current version 28 March 2024.

Digital Object Identifier 10.1109/ACCESS.2024.3375870

RESEARCH ARTICLE

A Novel Renewable Power Generation Prediction Through Enhanced Artificial Orcas Assisted Ensemble Dilated Deep Learning Network

ZHIFENG CHE¹, A. AMIRTHASARAVANAN², MUNA AL-RAZGAN³,
EMAD MAHROUS AWWAD⁴, MOHAMED YASIN NOOR MOHAMED^{5,6},
AND VAIBHAV BHUSHAN TYAGI⁷

¹Xinxiang Vocational and Technical College, Xinxiang, Henan 453000, China

²Department of Computing Technologies, SRM Institute of Science and Technology, Kattankulathur, Tamil Nadu 603203, India

³Department of Software Engineering, College of Computer and Information Sciences, King Saud University, Riyadh 11345, Saudi Arabia

⁴Department of Electrical Engineering, College of Engineering, King Saud University, Riyadh 11421, Saudi Arabia

⁵Department of Mathematics and Information Technology, Sultan Qaboos University, Seeb, Muscat 123, Oman

⁶Department of Electronics and Communication Engineering, Saveetha School of Engineering, Saveetha Institute of Medical and Technical Science, SIMATS University, Chennai, Tamil Nadu 600077, India

⁷Faculty of Engineering, ISBAT University, Kampala, Uganda

Corresponding author: Vaibhav Bhushan Tyagi (tyagi.fict@isbatuniversity.com)

This work was supported by the Deputyship for Research and Innovation, Ministry of Education, Saudi Arabia, under Grant IFKSUOR3-220-2.

ABSTRACT The different energy resource generation tends to have high-level variation, making the power supply complex for the end-users. Because of the intermittent nature, the variations occur by time, weather conditions, and output energy. Hence, this research aims to develop a new “Renewable Power Generation Prediction (RPGP)” model using Deep Learning (DL) to give the end user a reliable power supply. The data aggregation process initially accumulated the data in a normalized and structured format. Then, the data cleaning and scaling are performed to decrease the outliers and varying ranges of values. A higher-order statistical feature was attained from the cleaned and scaled data. This statistical feature was given to “Optimal Weight Computation Ensemble Dilated Deep Network (OWC-EDDNet)” to predict generated power. In this EDDLNet, networks such as “Recurrent Neural Networks (RNN), Long Short-Term Memory (LSTM), Deep Belief Networks (DBN), and Deep Neural Networks (DNN)” are employed to predict the renewable generated power. Finally, the prediction score attained from all deep networks is multiplied by the optimized weight to get the final prediction outcome, where the weights are optimally determined with the support of the Enhanced Artificial Orcas Algorithm (EAOA). The extensive empirical results were analyzed among traditional algorithms and prediction models to showcase the efficacy of the designed energy generation prediction scheme.

INDEX TERMS Renewable power generation prediction, enhanced artificial orcas algorithm, higher order statistical features, optimal weight computation ensemble dilated deep network.

NOMENCLATURE

| Abbreviations | Descriptions. | LSTM | Long Short-Term Memory. |
|---------------|--|------------|---|
| RPGP | Renewable Power Generation Prediction. | OWC-EDDNet | Optimal Weight Computation Ensemble Dilated Deep Network. |
| DL | Deep Learning. | DNN | Deep Neural Networks. |
| RNN | Recurrent Neural Networks. | DER | Distribution Energy Resources. |
| | | MG | Micro Grid. |
| | | ANN | Artificial NeuralNetwork. |
| | | DBN | Deep Belief Networks. |

The associate editor coordinating the review of this manuscript and approving it for publication was Ahmed F. Zobaa¹.

| | |
|---------|---|
| ELM | Extreme Learning Machine. |
| BLS | Broad Learning System. |
| CC-RNN | Cooperative convolution-based Recurrent Neural Network. |
| DGF | Double Gaussian Function. |
| SEA | Stacked Ensemble Algorithm. |
| RBFNN | Radial Basis Function Neural Network. |
| MASE | Mean Absolute Scaled Error. |
| DRNN | Deep Recurrent Neural Network. |
| ReLU | Rectified Linear Unity. |
| DeepMPC | Predictive Control. |
| GDBN | Growing Deep Belief Network. |
| QDRL | Quantum-Inspired Deep Reinforcement Learning. |
| AI | Artificial Intelligence. |
| ML | Machine learning. |
| SMAPE | Symmetric Mean Absolute Percentage Error. |
| CFO | CuttleFish Optimization. |
| FDA | Flow Direction Algorithm. |
| AOA | Artificial Orcas Algorithm. |
| EGSOA | Garter Snake Optimization Algorithm. |
| MEP | Mean Error Percentage. |
| RMSE | Root-Mean-Square Error. |
| MAE | Mean Absolute Error. |

Symbols Descriptions.

| | |
|------------|----------------------|
| P_g | Collected data. |
| P_g^{Ag} | Aggregated data. |
| P_g^{Fg} | Filled data. |
| P_g^{Cl} | Cleaned data. |
| P_g^{Po} | Pre-processed data. |
| P_g^{Sf} | Statistical feature. |

I. INTRODUCTION

Non-renewable energy resources depend on conventional electric power systems like coal, gas, and oil, which results in energy losses and greenhouse gases at the time of transmission and generation of electricity [1]. In the centralized grid station, a huge risk occurs when the large-scale energy transmission has some fault in mechanical or electrical areas [2]. The basis of “Distribution Energy Resources (DER)” is proposed to stop these challenges, improve reliable and stable power transmission to the end-user, and lower environmental impact. From the above range penetration, to use the energy storage units [3], The DER devices and sensors are effectively employed, and the proper local power generation integration assures the electricity grid based on the concept of “Micro Grid (MG)” [4]. It is designed to regain the utility system with contributors through cloud coupling. The MG system mostly overcomes the challenges in the conventional grid system, but new issues are created while managing the new MG settings in electricity [5]. These methods are generally based on energy harvesting resources, specifically solar and wind renewable power resources, where these sources are

mostly uncontrollable and unstable to continuous supply [6]. Also, electricity consumption affects consumer character and weather conditions [7]. In the literature, many advanced strategies are designed to predict the dispatch balance, electricity consumption, and supply, providing a consistent power supply [8].

Various studies offered different methodologies to approximate the dynamic characteristics of renewable resources to continue high accuracy [9]. In 2022, Kurdkandi et al. [35] have introduced the effective framework of transformer-less grid-connected inverters with two power diodes and six power switches that can produce six voltage stages at the outcome. In 2021, Marangalu et al. [36] have implemented a multilevel inverter-aided on flyback converter by utilizing the DC-DC flyback converter. In 2022, Marangalu et al. [37] have recommended an advanced switched-capacitor grid-tied inverter that diminished the leakage current utilizing the general grounded mechanism. In 2022, Vankadara et al. [38] have introduced an effective analytical model for the PV system under partially shaded conditions. The non-linear mapping techniques like “Artificial Neural Network (ANN)” are a better modeling technique for the complex systems. The great success achieved by the DL-based model is because of their better learning capability in approximating the dynamical characteristics of the energy resource. The maximum of the DL techniques is shallow models without a strong feature-extracting capacity [10]. The better predictive performance failed to be achieved when the plats input and output behavior is difficult. With the improvement of machine intelligence for the academic community, DL has the spotlight [11]. The cognitive process of the human brain is mainly based on knowledge from unsupervised feature extraction [12]. For the complex behavior of big modeling data, DL plays a better work than the other available models. Currently, the most successful DL model is the DBN mainly applied in computer vision. Specifically, the present years have identified DBN prospects in identifying, analyzing, and modeling nonlinear systems compared with another classical algorithm.

The successful prediction of the electric supply is the main focus of the present literature on the consumption and resources of renewable energy generation [13]. The state-of-the-art accuracy achieved by the hybrid model is based on DL for power consumption and generation prediction [14]. Various predictive designing methods are introduced to do these works, and the present model lacks a normalized method to achieve both operations at the time. Increasing the forecasting result is mainly focused by the researchers without considering the computational complexity of the technique [15]. For the electricity cost and losses, the great impact of predictive modeling is the reduction of error rate. The machine learning technique recently achieved huge progress in predicting and generating renewable power with other DL methods [16]. They are “Extreme Learning Machine (ELM), Broad Learning System (BLS), Cooperative Convolution based Recurrent Neural Network (CC-RNN), and DBN,” which attain good extraction of features from the modeling features and input

variables. Specifically, in 2022, Selvaraj et al. [39] have concentrated on very effective DL mechanisms for diagnosing the faults in solar panels. When comparing it with the baseline models, there is a lower complexity in the computational process, and the prediction result was higher for the designed framework.

The benefaction of the designed framework is detailed as follows.

- To create the renewable power generation prediction framework with a DL model that provides the effective outcome of reliable power supply.
- To get the pre-processed data by applying different operations, to remove the unwanted data thereby helping to improve the performance. To acquire the statistical features by considering the different measures like variance, kurtosis, skewness, and correlation coefficient, which represent the most essential features.
- To design the EAOA method that infers the concept of classical AOA algorithm to enhance the system performance and optimize weight to minimize the RMSE and MAE.
- To develop an OWC-EDDNet model for predicting the power generation. Here, this network is modelled with DBN, LSTM, RNN, and DNN in that the final predicted value is estimated by computing the optimal weights with the help of the proposed EAOA, thereby assisting in enhancing the system's efficiency.
- To examine the effectiveness of the implemented method by employing numerous measures and contrasting it with diverse existing conventional techniques and optimization systems.

The framework of the suggested framework is given here. Module II offers the traditional models of the suggested work. The framework of PGP using DL is presented in Module III. Module IV explains the data cleaning and higher-order statistical features. The prediction using an ensemble dilated DL network is demonstrated in Module V. The solutions and explanation of the proposed framework are displayed in Module VI. Finally, module VII concludes the designed framework.

II. EXISTING WORKS

A. RELATED WORKS

In 2021, Ahmed Khan et al. [17] have designed a PGP technique based on DL. Here the generation of different energy resources got a high-level variation, which was more challenging for the end-user to make a reliable power supply. Due to the variation of time in weather conditions and energy output based on the intermittent nature, the variations occur. The present literature focuses the power consumption prediction and generation of power. This demands a smooth smart grid present operation with balanced energy consumption and generation for the connected customers. The effective and efficient hybrid model was developed for forecasting consumption and power generation and supported energy

harvest by offering powerful predictions for renewable energy analysis. The conventional neural network with an echo state model was used to forecast consumption and energy generation. The meaningful pattern extracted from the historical data using a convolution network was then forwarded to temporal feature learning. The resultant spatiotemporal feature was sent to a fully connected layer for the end prediction. The sustainability of the recommended model decreased the forecasting faults using “MSE, MAE, RMSE and NRMSE metrics” compared to the “state-of-the-art model between the consumers and production resources.

In 2021, Khan et al. [18] have initiated automatic power forecasting in renewable energy resources. For renewable energy, high-level integration was important to forecast accurate solar energy that controls the electricity grid. In the unprecedented granularities of the present data, there was the chance to utilize a data-driven algorithm for developing solar generation prediction. By using the LSTM and ANN” the improved “Stacked Ensemble Algorithm (SEA)” was produced for the prediction of solar energy. With the highly gradient boosting algorithm, the base model prediction was integrated to improve the correctness of the prediction generation of solar PV. The designed framework estimated 4 solar generation resources for a detailed estimation. In addition, it offers a thorough knowledge of the learning strategy by utilizing the additive explanation framework. The value of the implemented method was determined by contrasting the prediction result with single LSTM, Bagging, and ANN. As a result, the developed DSE-XGB model exhibited better consistency combination and stability.

In 2019, Hong et al. [19] have introduced the renewable energy power generation resource based on the DL method. The fluctuation of wind speed was based on the generation of wind power associated with uncertainty. The more important factor for efficient power system tasks was an effective forecasting of wind power creation. This hybrid model depends on the CNN, which cascaded “Radial Basis Function Neural Network (RBFNN) with Double Gaussian Function (DGF)” as its activation function. The wind power behavior was extracted using the CNN by the pooling operation, kernel, and convolution. The DGF incorporated RBFNN with uncertain behaviors. The wind form measured the realistic wind power generation used in the simulation. By using the “Tensor Flow and Keras Library,” the developed method was introduced. The solution revealed the simulation of the implemented framework was more accurate than the traditional models.

In 2022, Shabbir et al. [20] have implemented a new method using energy prediction based on DL in the renewable energy resource. Due to the number of factors, the stability of the wind energy was featured based on the “season, climate area, weather and time of the day”. Further, new challenges were started from the instability of the wind energy to the electric power grid like flexibility, power quality, and Reliability. The transition required advanced techniques for predicting wind energy for accurate forecasting. DL and machine learning closely tied the wind energy prediction to

form the intelligent energy management paradigm. The short-term wind energy prediction issues were attempted in this article using historical wind energy generation data. Also, various trending DL algorithms were implemented for the day-ahead prediction. The elaborated exploratory analysis was conducted for the selection of system attributes. The Estonian wind energy real-time creation resource trained all the models with a frequency of 1 hour for the first time. For Estonia, fostering an efficient forecasting technique was the main objective. The result of the comparative analysis showed the implemented method was more efficient when compared with the TSO forecasting algorithm. Therefore, the effective computation and more suited method in DL was the RNN-LSTM for forecasting wind energy in Estonia.

In 2022, Alshammar et al. [21] have proposed a renewable energy forecasting resource using DL. Renewable energy sources remain important substitutes for the standard generating of undeniable energy. The deployed wind power capacity presented half the capacity compared to other replenished power sources. Wind power generation results from the seasonality and changeability in the “direction, humidity, atmospheric pressure, precipitation, and wind speed”. The “Deep Recurrent Neural Network (DRNN)” was employed for establishing the prediction of wind speed, hence, applied the multi-step and single-step DRNN. The “Mayfly Optimized DRNN (MO_DRNN)” regards the activation functions like “Rectified Linear Unity (ReLU) and Stacked CNN (SCNN)”. The proposed MO-DRNN method minimized the error rate of the FS procedure.

In 2020, Wang et al. [22] have suggested energy prediction based on the DL method. The “Continuous Stirred-tank Reactor (CSTR)” was largely utilized in wastewater treatment. Due to the high difficulty of attaining accurate system identification, the industrial process control problem was challenging. To control the CSTR system, the “Deep Learning based Model, Predictive Control (DeepMPC)” was proposed in the work. The developed DeepMPC contained a “Growing Deep Belief Network (GDBN)” and the optimal controller. At first, the size was determined automatically by the GDBN to attain maximum performance with transfer learning in the system identification. For the controller system, it acts as a predictive model. The controller’s dynamic accurately approximated the model with the regular, ultimately bounded error. The quadratic optimization was conducted in the second phase to obtain the optimal controller. Here the convergence and stability of DeepMPC were determined. In the end, the second-order CSTR system was controlled and modeled by the DeepMPC. From the result, the DeepMPC showed better modeling, anti-disturbance, and tracking performance than another baseline method.

In 2021, Qian et al. [23] have initiated the energy prediction technique based on a DL model. The reliable power supply of different energy generations with high-level variation was significantly hard for the end user. Because of the intermittent characteristic of time-changing weather situations and energy output, the variation occurs. The recent focus of the

literature was the improvement in forecasting consumption and power generation, which demands the smooth operation of the present smart grids with the consumption and generation of energy for related customers. Motivated by the load prediction application, suggested the effective and efficient model for predicting the consumption and generation of power contributing to the energy by offering high forecasting information to analyze the renewable energy. The echo state network with CNN was employed to forecast the consumption and creation of the renewable energy. The CNN extracted the significant features from the previous information, which were subjected to the echo stage network for learning the temporal feature. The resultant feature vector was sent to the fully connected layer for the prediction. After the extensive experiment, the implemented framework was modeled over the “DL and machine learning technique”. Here the result showed the suggested framework minimized the prediction faults by employing various measures.

In 2023, Thejus et al. [24] have introduced a DL-based pattern model for renewable energy power prediction with carbon emission. The challenge was attaining carbon neutrality and real-time distributed management for renewable energy devices. Here was the “Quantum-Inspired Deep Reinforcement Learning (QDRL)” with a multi-agent approach for real-time distributed creation control the renewable energy. Here the DRL approach was compared with nine QDRL approaches under two RES. The QDRL contained more frequency deviation and minor carbon emission, obtained from the numeric result under the complex RES. The state of prosumers matched the quantum state of QDRL. The result verified that the multi-agent method controlled the real-time control problem for QDRL exploration and exploitation.

B. RESEARCH GAPS AND CHALLENGES

The wide range changes of in distinct energy creation resources make a sufficient power supply very difficult for the end-users. These changes happen because of the intermittent characteristics of the time-changing weather situations and the energy outcome. Therefore, a new DL-based renewable PGP model is introduced to win over the challenges. The features and challenges of renewable PGP systems are given in Table 1. CNN [17] can produce high accuracy in prediction and provides sufficient energy transmission by matching the consumption and generation of power. Yet, an enormous amount of labeled data is demanded to train the variables, and is time-consuming. ANN and LSTM [18] can handle more than one task simultaneously and provide permanent memory for storing the data. But, the small variation in the given data may lead to substantial changes in the forecasting values that also trouble the model’s reliability. RBFNN [19] tolerates input noises and can handle high-dimension and non-linear data. But, slow computation leads to training difficulties and high adversarial attacks, which leads to misclassification in DL models. RNN-LSTM [20] can approximate arbitrary non-linear systems with high precision. But, the model’s

TABLE 1. Features and challenges of existing deep learning-based renewable power prediction systems.

| Author [citation] | Methodology | Features | Challenges |
|-----------------------------|----------------|--|---|
| Harrou <i>et al.</i> [18] | VAE-based 1SVM | <ul style="list-style-type: none"> It has the speed and accuracy for processing vast volumes of medical imaging information. It can support options for therapy by forecasting the results for patients. | <ul style="list-style-type: none"> Understanding the internal operations of this model can be challenging, which makes it more challenging to comprehend the reasoning behind certain conclusions. |
| Ayal <i>et al.</i> [19] | Mini-COVIDNet | <ul style="list-style-type: none"> It has the ability to identify minute patterns and details in medical imaging that an ordinary observer could overlook. | <ul style="list-style-type: none"> It needs sophisticated technology to function well and may become computationally costly. |
| Oyelade <i>et al.</i> [20] | CovFrameNet | <ul style="list-style-type: none"> This model can be combined with additional diagnostic instruments to improve precision all around. It may be applied to populations at increased risk for purposes of screening. | <ul style="list-style-type: none"> Because it relies on imaging information, it could not be capable of identifying COVID-19 in situations where imagery is either unavailable or not widely used. |
| Romaissa <i>et al.</i> [21] | DnCNN | <ul style="list-style-type: none"> It can lessen the strain on medical personnel. It can be utilized to track the COVID-19 outbreak through surveillance. | <ul style="list-style-type: none"> But it remains susceptible to errors such as false positives as well as false negatives, which could result in absences or incorrect diagnoses. |
| Kumar <i>et al.</i> [22] | SCovNet | <ul style="list-style-type: none"> It can support the creation of vaccinations and tailored treatments. It could enhance the efficacy as well as efficacy of COVID-19 treatment and diagnosis. | <ul style="list-style-type: none"> Image excellence, decision, and turbulence are some of the elements that might affect the accuracy of CNN's simulations. |
| Devi <i>et al.</i> [23] | CNN | <ul style="list-style-type: none"> It can deliver objective, steady outcomes while lowering the possibility of error by humans. | <ul style="list-style-type: none"> There could be biases in identification if this model does not extend effectively to other demographics or different types of imaging. |
| Prakash <i>et al.</i> [24] | COVID-SSNet | <ul style="list-style-type: none"> It can be utilized to ensure accurate and dependable outcomes in medical imaging quality control. | <ul style="list-style-type: none"> It might not have been capable to manage ambiguity properly, which could cause detection findings to be overestimated or underestimated. |
| Ahuja <i>et al.</i> [25] | CNN | <ul style="list-style-type: none"> It can be used to improve the availability of medical equipment in rural or resource-constrained places. It can assist in prioritization and assessing clients, giving people who are more vulnerable priority. | <ul style="list-style-type: none"> The accuracy and uniformity of the diagnostic imaging information applied to train can have an impact on a CNN's effectiveness. |

Reliability, flexibility, and power quality are low, and the vanishing gradient problem is high in this model. DRNN and SCNN [21] reduce the overfitting issue, and the issue regarding lower training rates is reduced by using this model. Yet, the performance is limited and affects the privacy and security of data. GDBN [22] computation expense is very low because the layers are linearly connected in the network with a feed-forward mechanism. Even though the hardware requirements are so expensive and complex, and huge amount of data is needed for the computation. CNN with Echo state [23] have a simple training model and better modeling ability to solve the overfitting problem in the network. But, it does not apply to real-world scenarios of collection of data. QDRL [24] is used for real-time distribution of energy and generation, and

reinforcement learning is used to solve complicated tasks with less prior information. But, it produces overload in the network, which affects the accuracy of the result, and the maintenance cost is also high. Therefore, the issues addressed in the conventional approaches pave the way to develop a new DL-based energy consumption prediction model.

C. MOTIVATIONS

The conventional renewable power prediction approaches didn't extract the significant features from the original data that included more outliers. This leads to inaccurate predictions. Generally, the input data contains lots of noise and outliers. These are removed by the operation called pre-processing. However, most of the conventional works

didn't pre-process the data during the prediction process. This reduced the effectiveness of the model. Hence, the developed model initially, pre-processed the data before predicting the data. Also, considering the significant features for accurate power prediction improves the correctness of the outcome.

Hence, the implemented framework utilized the feature extraction process. A lot of the conventional works failed to utilize this process. Further, some of the conventional techniques utilized single techniques to predict the. This reduced the efficacy of the model. Hence, this presented work utilized various powerful DL techniques to predict renewable power with low error rates. Moreover, the implemented model highly minimized the power consumption, processing time, cost, and hardware requirements. Moreover, this model provides a reliable and robust framework.

III. INTELLIGENT MODEL OF RENEWABLE POWER GENERATION PREDICTION USING ENSEMBLE-BASED DEEP LEARNING MODEL

A. EXPLAINING THE RECOMMENDED METHODOLOGY OF POWER GENERATION PREDICTION

Due to the growth of the economy and population, there is a sudden increase in power consumption, which requires the demand for energy resources. The exceeding demand depletes conventional fossil resources of electrical energy. At the same time, renewable source wind energy has rapidly developed and received global attention. Wind energy reduces the pressure of energy demand and provides clean energy, highly reducing environmental pollution. The high-technology wind PGP affects the power grid, stability, power quality, and balance between power generation and load power grid processing. It is the major significant for efficient operation, stability, and security. Due to the non-linear wind speed behavior, the correct forecasting of the power creation is a difficult task, which has a high rate of changes with no typical patterns and mostly depends on separate atmospheric temperature and pressure. This non-linear characteristic of wind speed makes extracting features and accuracy in wind power creation forecasting difficult. Because of the conventional neural network's capacity to overcome issues like higher time in training and minimum convergence, the DL method is getting high attention among researchers. Because of the improvement and development in the sector of "Artificial Intelligence (AI) based prediction, "Machine learning (ML) and DL have successful tools for resource energy prediction. More forecasting methods to predict power generation include statistical models, physical methods, ANN, and hybrid intelligent methods. Other prediction models, such as the restricted Boltzmann machine, LSTM, auto-encoder, and CNN, have been used to predict wind power creation. Because of the unpredictable, irregular, and inconsistent character of the resource energy data, consumption forecasting and energy generation remain difficult tasks. In contrast to the traditional approaches, the DL approach for time series

prediction often lacks interpretability. This is one of the most challenging issues when applying those approaches in practice. To overcome such limitations, EAOA is proposed to predict the wind power forecasting is presented in Figure 1.

The new prediction framework for renewable power generation is developed according to the DL to provide a continuous power supply to the end user. At first, the data accumulated by the data aggregation in the structured and normalized format. Data scaling and cleaning are performed to reduce the changes in the value range and outliers. From this process, a higher-order statistical feature was achieved. Then the OWC-EDDNet helps to predict the generated power from the statistical feature. In this network, "RNN, LSTM, DBN, and DNN are employed to forecast renewable power generation. The optimal weight is multiplied by the prediction score result from the deep networks to attain the forecasting result. Here the weights are optimized with the help of developed EAOA. Among the classical algorithms, the extensive empirical result was determined and forecast the effectiveness of the suggested energy generation forecasting method.

B. DATASET DETAILS

The solar power creation and sensor information for two power plants is utilized from the link:

"<https://www.kaggle.com/datasets/anikannal/solar-power-generation-data>: access date: 2023-08-08". The two solar power plant data over 34 days were collected. From the power generation data, the gathered data is represented by P_g , where $g = 1, 2, \dots, G$ and G is the obtained data.

C. DATA AGGREGATION

Data pre-processing is the most important and influential for generalization performance for the prediction process. Data aggregation is the first phase of data preprocessing. The gathered data from the dataset P_g are given as input here. The significant concept of data aggregation is to group all the gathered data. Here, the aggregation combines the data from different sources with various formats into coherent recompilation, generally into a database. Aggregation takes place for the same type of data with multiple problems. The aggregated data from this phase is denoted as P_g^{Ag} .

IV. DATA CLEANING AND SCALING, HIGHER ORDER STATISTICAL FEATURES, AND IMPROVED HEURISTIC ALGORITHM FOR PREDICTION

A. DATA CLEANING AND SCALING

The data aggregate output from the previous phase is input to data filling. The missed value and characters in the data decreased the model's effectiveness. Here the output data P_g^{Ag} from the data aggregation is given as input. Here the original data is reformed by filling in the missed character and data values. The output obtained from the data filling is denoted as P_g^{Fg} .

Data Cleaning is the third phase of data pre-processing. Here the output from the data filling P_g^{Fg} is introduced as

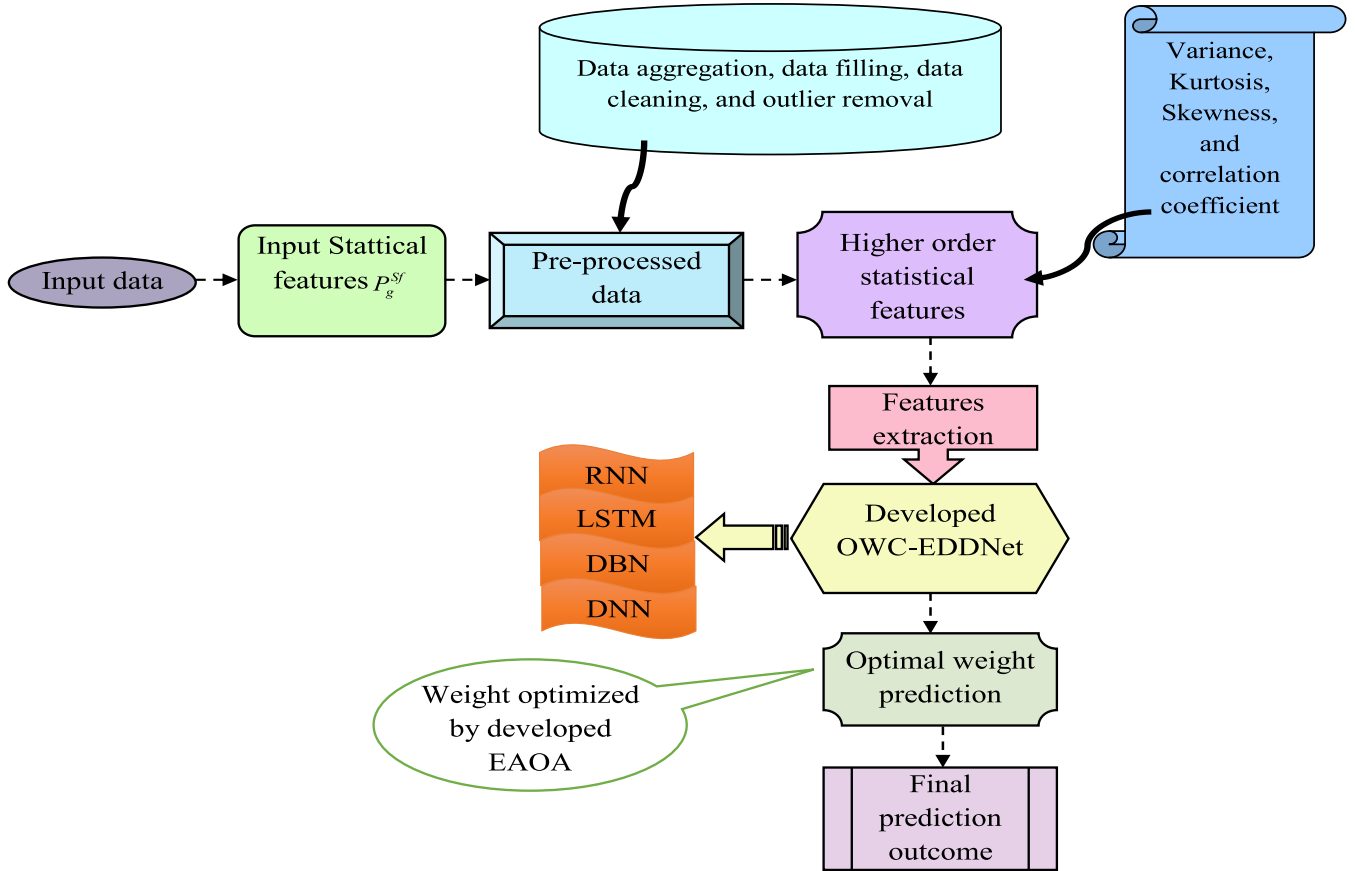


FIGURE 1. Diagrammatic view of power generation prediction model using developed EAOA.

input. In this method, the data were organized and corrected, free from inaccuracy, messy, and poorly formatted data. The cleaned data is obtained from the data cleaning process and denoted as P_g^{Cl} .

The final phase of data preprocessing is the outlier removal. Here the cleaned data output P_g^{Cl} is given as input. In this phase, the problematic outliers from the collected data are eliminated, which causes poor sampling, measurement error, and processing errors. The output from the outlier removal is the pre-processed data, represented as P_g^{Po} .

B. HIGHER ORDER STATISTICAL FEATURES

In order to extract the feature from the pre-processed data, higher-order statistical measurements are employed. In this phase, the pre-processed data P_g^{Po} fed into statistical feature extraction. Here “variance, kurtosis, skewness, and correlation coefficient,” are utilized in this process.

1) VARIANCE

The average square variation between the whole data point and the center of the distribution measured by the average is shown in Eq. (1)

$$Var = \frac{\frac{1}{n} \sum_{i=1}^n (P_g^{Po} - \bar{g})^2}{\sum_{i=1}^n (P_g^{Po} - \bar{g})} \left(\frac{1}{n} \sum_{i=1}^n (P_g^{Po} - \bar{g})^2 \right)^2 \quad (1)$$

2) KURTOSIS

It explains the peak relative sharpness to a normal distribution in a frequency distribution curve shown in Eq. (2)

$$Kur = \frac{\frac{1}{n} \sum_{i=1}^n (P_g^{Po} - \bar{g})^4}{\left[\frac{1}{n} \sum_{i=1}^n (P_g^{Po} - \bar{g})^2 \right]^2} \quad (2)$$

3) SKEWNESS

This method determines the symmetry measures. The dataset is symmetrical when the right and left sides of the central point are similar. The skewness is defined in Eq. (3)

$$Ske = \frac{\frac{1}{n} \sum_{i=1}^n (P_g^{Po} - \bar{g})^3}{\left[\frac{1}{n} \sum_{i=1}^n (P_g^{Po} - \bar{g})^2 \right]^{3/2}} \quad (3)$$

4) CORRELATION COEFFICIENT

It is the calculation of the relationship between two measures. It describes each other’s by utilizing the measures equated in Eq. (4)

$$Cor = \frac{\frac{1}{n} \sum_{i=1}^n (P_g^{Po} - g)(h_i - \bar{h})}{\sqrt{\frac{1}{n} \sum_{i=1}^n (P_g^{Po} - \bar{g})(h_i - \bar{h})^2}} \quad (4)$$

5) SPECTRAL CENTROID

It is the frequency spectrum average amplitude weight which related to the brightness or human perception of the instrument. The Spectral centroid is formulated in Eq. (5)

$$SpC = \frac{\sum_{i=1}^n |P_g^{Po}(g_i, g_i)|g_i}{\sum_{i=1}^n |P_g^{Po}(g_i, g_i)|} \quad (5)$$

6) SPECTRAL FLUX

It is the calculation of total spectral changes. This is determined by the difference between successive frames of normalized magnitude spectra and given in Eq. (6).

$$Spf = \left(\sum_{i=1}^n |P_g^{Po}(g_i, g_i) - P_g^{Po}(g_{i-1}, g_{i-1})| \right) \quad (6)$$

Here the initial statistical data is P_g^{Po} which is obtained from the preprocessed data. \bar{g} is the main probability attained value, n is the count of the value. h_i is the value present in the given data. g_i frequency related to every magnitude element. In the final, the statistical data is extracted as a feature and termed as P_g^{Sf} .

C. PARAMETER TUNING USING EAOA

Here the suggested algorithm, EAOA, is employed for parameter optimization to enhance the prediction outcome. The optimization is designed based on traditional AOA. The merits of using AOA can solve the hard problem and yield the best success rate. Also, to improve the efficiency of AOA, an implementation of a random factor r in Eq. (17) for the recommended EAOA is expressed in Eq. (7).

$$r = \frac{(bestfit * currentfit)}{(worstfit * currentfit)} \times 2/3 \quad (7)$$

AOA [25]: It is based on the resident orca's manner of living and their characteristics. To attain the prey, the orcas use unique, diverse techniques. By using their collective intelligence, they move to catch the easy prey. Orcas use echolocation for the tough once before hunting. This characteristic of the hunting method and echolocation mechanism is simulated in the AOA in the exploitation phase. The female orcas, independent after the descent, simulate the exploration phase. The mechanical formation of the algorithm is explained below.

Modeling collective motion: The orcas avoid collision by moving in such a way with the neighboring flock mates. This is to order the velocity of the nearest flock mates and be in the center of the flock. The motion of the orca is based on the present speed of the nearby pod performance of the clan of their own. The algorithm simulates this behavior for searching for the optimal outcome in the large search place. At the given time, the orca is simulated by each solution, which evolves to the optimal solution. It is separated by the velocity that evaluates the fitness function, directs its motion, and measures the performance with an optimal solution. The group of artificial orcas initializes the process, aiming to find the best solution. It renews various iterations in the search space until the end of seeking the optimal solution with the

best quality. The entire orca upgrades its speed at all iterations and the place is based on its clan mates to find the congeners in the swarm. The updating of the orcas is expressed in Eq. (8)

$$w_i^t = x_i w_i^{t-1} + x_{Q_i} * e(y_{Q_i}^*, y_i^{t-1}) + x_{d_i} * e(y_{d_i}^*, y_i^{t-1}) \quad (8)$$

Here $y_{Q_i}^*$ is the best position, $y_{d_i}^*$ is the best solution by the orca in the clan d_i . w_i^{t-1} is considered as the velocity of the orca at the period $t - 1$. x_{p_i} is the social skill of the orca that belongs to the pod Q_i . The significance of the orca simulates the pod, and the determination is given in Eq. (9). Eq. (10) also calculates the orca skill, which belongs to the contribution of the separate clan.

$$x_{Q_i} = \frac{g(y_i^{t-1})}{\sum_{j \in Q_i} g(y_j^{t-1})} \quad (9)$$

$$x_{d_i} = \frac{g(y_i^{t-1})}{\sum_{j \in d_i} g(y_j^{t-1})} \quad (10)$$

Here the factor x_{d_i} is the orca's social skill $g(y)$ is the fitness function of the solution y . The term y_i^t is the orca position at the time t , expressed in Eq. (11)

$$y_i^t = w_i^t + y_i^{t-1} \quad (11)$$

The motion of the water wave to take the single will take wave forward, which is determined in Eq. (12)

$$y_i^t = \gamma * \left(\sin \frac{2\pi}{M} y_i^t - \frac{2\pi}{M} t \right) \quad (12)$$

Here γ is the wave amplitude with the empirical parameter. The factor M is the wavelength and T is the period. Thus, $T = 1$ and $M = s * T = s$. The term s is the sound speed and t is the time for a wave during all iterations. If this stage does not end with the optimal solution, then the echolocation stage occurs.

Modeling Echolocation: Orcas generally use echo location that has a strong sound impulse emission and allows the surrounding object perception. The vibration in the sound crosses the water and brings the prey information. The orca uses high speed and is designed according to the behavior of the echolocation mechanism. In the first phase, every individual in the population returned with frequency and loudness. The variation of frequency between the parameters is g_{\min} and g_{\max} which described in Eq. (13)

$$g_i^t = g_{\min} + (g_{\max} - g_{\min})\beta \quad (13)$$

Here, β is the random factor in the limit $[0, 1]$. The orca's loudness is highly strong at the start of echolocation; it reduces when it is near the prey. It changes from positive to minimum value formulated in Eq. (14)

$$B_i^t = \delta B_i^{t-1} \quad (14)$$

Here δ is the empirical parameter, which reduces in all iterations. The velocity of the same loudness expressed in Eq. (15)

and Eq. (16) determines the iteration to improve the matriarch position.

$$w_i^t = \frac{1}{g_i^t} B_i^t \quad (15)$$

$$y_i^t = w_i^t + y_i^{t-1} \quad (16)$$

The Narrowing Enriching Mechanism: Here, at all iterations, orcas reduce the size of the circle and shrink to separate distance from prey. Here the term r is the random factor which is modified in the proposed EAOA from Eq. (7) to improve the efficiency of the implemented method. The first position of orcas is modified in Eq. (17), and the reduced circle for iteration is shown in Eq. (18)

$$y_i^t = \begin{cases} y_i^{t-1} + e(y_i^{t-1}, y^*) - s & \text{if } e(y_i^{t-1}, y^*) > r \\ y_i^{t-1} + s - e(y_i^{t-1}, y^*) & \text{otherwise} \end{cases} \quad (17)$$

$$y_i^t = y_i^{t-1} + r - b \quad (18)$$

For the Archimedes spiral motion, the orcas place themselves at a similar distance, and the simulation is expressed in Eq. (19)

$$y_i^t = y_i^{t-1} - 2\pi m \quad (19)$$

Between the enriching narrow mechanism, the probability α is chosen, and the spiral design upgrades the place of orcas in Eq. (20)

$$y_i^t = \begin{cases} y_i^{t-1} + r - b & \text{if } q < \alpha \\ y_i^{t-1} - 2\pi m & \text{otherwise} \end{cases} \quad (20)$$

Exploration Stage: With the characteristic of the female resident orcas leaving the family, the exploration phase brings out the arbitrary matriarch from the clan. Based on the capacity, it creates a different new population from the old one. It helps to prevent premature convergence. The new position is formulated in Eq. (21)

$$y_{new}^* = y^* + \text{MaxDistance}(y^*) \quad (21)$$

Here y^* is the selected matriarch, y_{new}^* is the new position, $\text{MaxDistance}(y^*)$ and is the matriarch distance according to the capacity.

The pseudocode for developed EAOA is presented in Algorithm 1.

The flowchart for the implemented IKOA technique is represented in Figure 2.

V. PREDICTION USING ENSEMBLE DILATED DEEP LEARNING NETWORK USING OPTIMAL WEIGHT COMPUTATION

A. NETWORKS USED IN ENSEMBLE

EDDNet contains a multilayer neural network that progressively extracts the feature from the input data and produces predicted output based on the features. The feature extracted data from the higher order statistical feature P_g^{Sf} is given as input to every below network for the predicted outcome.

Algorithm 1 EAOA

Initialize the parameter of EAOA.

Calculate the population and highest iteration value

Consider the arbitrary factor as r

While the iteration commences

If $r = \frac{(\text{bestfit} * \text{currentfit})}{(\text{worstfit} * \text{currentfit})} \times 2/3$

EAOA is processed

Upgrade the best outcome

Calculate the fitness value of all individuals.

Generate the population for a new place in Eq. (21)

End if

End

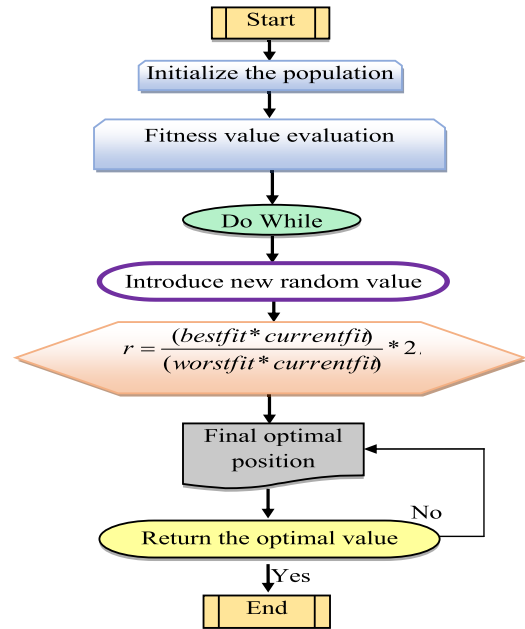


FIGURE 2. Flow chart for proposed EAOA.

DRNN [31]: The variants of RNN are used classically for different sequential learning problems. The gradient problem of temporal dependencies inhibits their learning range and has minimum computational efficiency. The feature P_g^{Sf} is given as input to DRNN, which is the cell-independent, multilayer variant of RNN, which overcomes the challenges of computational efficiency and flexibility according to the RNN block of the neural network. Here, the single-layer and parallel skip connections minimize the sequence length. And also increases the computational cost when compared with traditional RNN. The information flow connection among the layers skips by the dilation by avoiding specific timestep equated in Eq. (22)

$$d_u^{(m)} = g(y_u^{(m)}, d_{u-t^{(m)}}^{(m)}) \quad (22)$$

Here $d_u^{(m)}$ is the cell in a layer m at the time u . $t^{(m)}$ is the skip length and $g()$ is the RNN operation. Here, the earlier cell state depends on regular skip connection is deleted for effective dependence on a skipped cell stage. This effectively handled the existing gradient problem. The dilation of the m^{th}

layer $t^{(m)}$ determined in Eq. (23)

$$t^{(m)} = N^{m-1} \quad (23)$$

By using the mean recurrent length, the efficiency of DRNN qualified and measured the average dilations.

DLSTM [32]: LSTM is a modern kind of RNN with the learning capability of long-term dependencies in sequential data. The general LSTM block contains a memory cell, which maintains the nonlinear regulator called gates. It helps the flow of data controls in the block. In the LSTM block, there are hidden states and cell states. The data from the historical time sequences is in the cell stage. The gate helps to ignore or add data to the cell stage. The gates are input, output, and forget gate. Each time step uses the previous state of the network. Here the input P_g^{Sf} helps to determine the output and update the cell stage. The hidden stage controls all the gates and the input. The dilated expression of the mathematical LSTM block with the time step is in Eq. (24).

$$d_t^m = g_t^m \otimes d_{t-1}^m + j_t^m \otimes h_t^m \quad (24)$$

Here t is the time step, \otimes is the element-wise product that refers to the first layer of the DLSTM model with the standard LSTM block. The timestep with the hidden state is expressed in Eq. (25)

$$i_t^m = p_t^m \otimes \sigma_d(d_t^m) \quad (25)$$

Here, σ_c is the state activation function, which is referred to as a hyperbolic tangent function. The determination of gates is shown in the below Equations.

$$g_t^m = \sigma_h(X_g^m y_t + W_g^m i_{t-1}^m + c_g^m) \quad (26)$$

$$j_t^m = \sigma_h(X_j^m y_t + W_j^m i_{t-1}^m + c_j^m) \quad (27)$$

$$h_t^m = \sigma_d(X_h^m y_t + W_h^m i_{t-1}^m + c_h^m) \quad (28)$$

$$p_t^m = \sigma_h(X_p^m y_t + W_p^m i_{t-1}^m + c_p^m) \quad (29)$$

Here X , W and c are the input weight, recurrent weight, and biases σ_h are the sigmoid gate activation function. A DLSTM block receives the input gate but not the previous one d_{t-1} and i_{t-1} but the old state d_{t-e} and i_{t-e} where $e > 1$ is a dilation. The hierarchical dilation is stacked with multiple dilated layers to construct the system to increase the ability to learn long-term dependence from different domains. For some seasonal time series, the DLSTM is useful where the series element has a cyclic character. This character model is incorporated by dilation related to seasonality.

DDBN: DBN [33] in machine learning is more famous based on the semi-supervised learning method. It contains two state learning processes supervised learning followed the unsupervised learning. The weight and biases were evaluated using the unsupervised stacked ‘‘Restricted Boltzmann Machines (RBM)’’ between the visible and hidden layers. Two adjacent layers, which are hidden layers stacked in the RBM layer. RBM connection with adjacent nodes, which is an energy-based function. The fine-tuning supervision followed the pre-training with the biases and weighted neurons to increase the parameters.

The specialized model of DBM has a hidden layer of DL. More dilation and descriptive features are held in the upper layer to find the solution. DBN has the advantage of achieving high performance with a minimum number of training sets compared with other classical neural networks. Using fine-tuning, the weights and biases are updated to enrich the model’s correctness. The probabilistic of DBN with input P_g^{Sf} determined in Eq. (30)

$$Q(y, i^1, \dots, i^m) = \left(\prod_{l=0}^{m-2} Q(i^l | i^{l+1}) \right) Q(i^{m-1}, i^m) \quad (30)$$

Here $Q(i^{m-1}, i^m)$ is the conditional distribution between the nearby layers and i^0 is the input vector. The energy function for (i^{l-1}, i^l) expressed in Eq. (31)

$$F(i^{l-1}, i^l; \theta) = - \sum_{u=1}^{E_{l-1}} \sum_{t=1}^{E_l} x_{ut}^l i_u^{l-1} i_t^l - \sum_{u=1}^{E_{l-1}} c_u i_u^{l-1} - \sum_{t=1}^{E_{l-1}} c_t i_t \quad (31)$$

Here $\theta = (x_{ut}, c, d)$ are the parameters of DBN x_{ut} is the weight among u^{th} neurons in the layer i^{l-1} and t^{th} neurons in i^l layer. The distribution energy function is expressed in Eq. (32)

$$Q(i^{l-1}; \theta) = \frac{\sum_{i^l} \exp(-F(i^{l-1}, i^l; \theta))}{\sum_{i^{l-1}} \sum_{i^l} \exp(-F(i^{l-1}, i^l; \theta))} \quad (32)$$

The weight is refined using supervised learning on gradient descent. This fine-tuning process has obtained a higher classification performance. The DDBN model is formed by using the dilated on traditional DBN. The dilated [40] convolution is incorporated into the traditional DBN network. It increases the effectiveness of the DBN network. Moreover, DDBN has demonstrated the prediction task to improve accuracy. It acquires more information by a large receptive field, and the output includes a wide amount of feature data. The dilation expands the receptive field to capture more information.

DDNN: The DNN [34] consists of an input variable, output variable, and weights. The amount of processing units made the layers in the DNN. The feature P_g^{Sf} is fed into the first layer. Depending on the structure second layer is the hidden layer. And then the final layer is the output layer which depends on the activity of the hidden layer. The process of trial and error specifies the neurons and layers. In every iteration, the DNN training phase is updated according to Eq. (33)

$$x_{kj} = x_{kj} + \eta \delta_k y_{kj} \quad (33)$$

Here y_{kj} is the input unit, x_{kj} is the j^{th} input weight, η is the learning rate. The output layer δ is upgraded utilizing Eq. (34) and the hidden layer δ is upgraded utilizing Eq. (35).

$$\delta_l + p_l(1 - p_l)(u_l - p_l) \quad (34)$$

$$\delta_i + p_i(1 - p_i) \sum_{l \in output} x_{li} \delta_l \quad (35)$$

Here P_l and P_i is the generated output with the hidden unit. u_l is the target output between the number of hidden layers. The

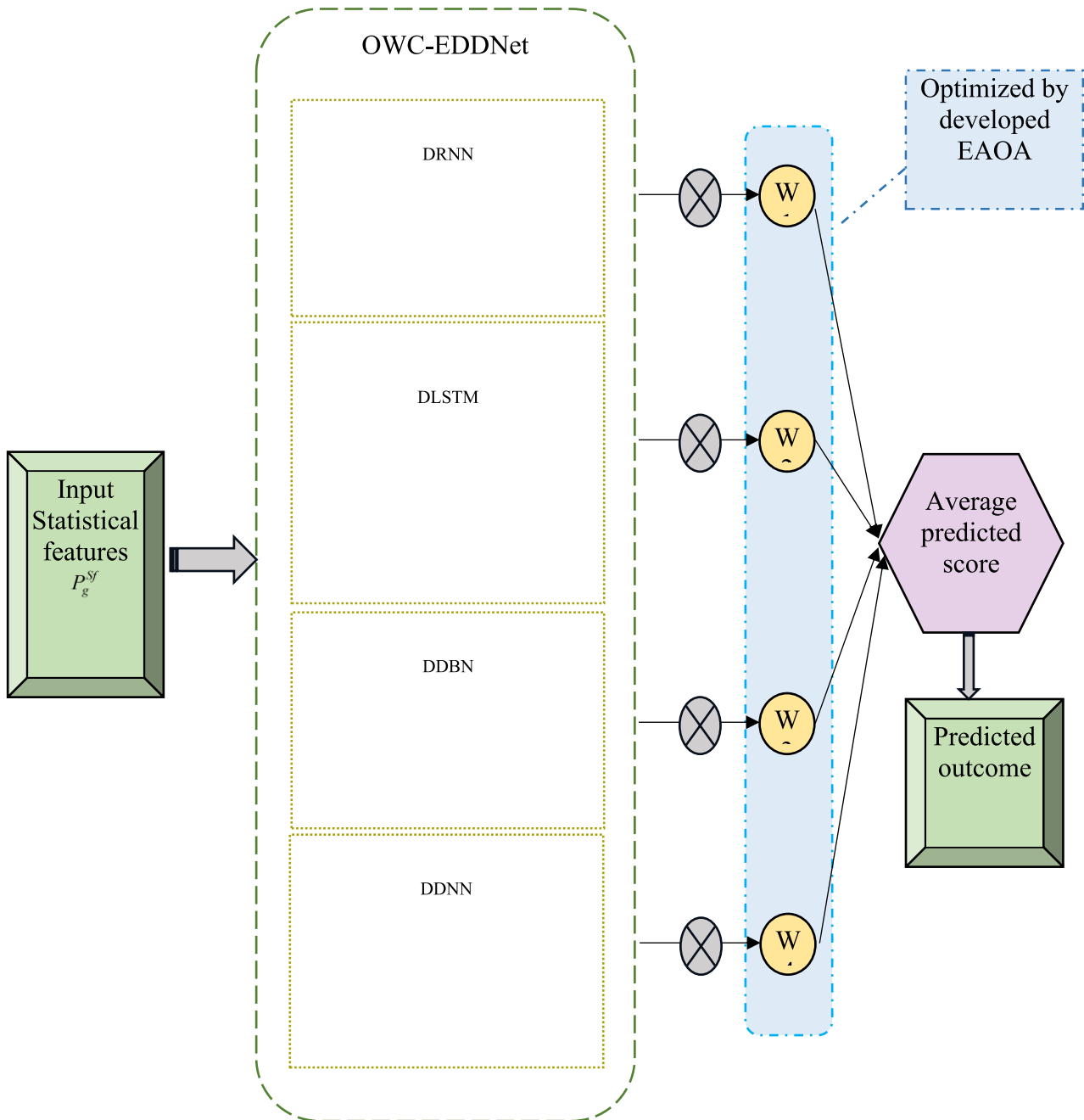


FIGURE 3. Structural view of developed OWC-EDDNet.

DNN modifies itself to use the filter parameters in various ways to form a DDNN. Here also, the dilated convolution [40] is utilized to construct the DDNN. The DDNN applies the same filter at various ranges for different dilation factors. The proper implementation of the dilated operator does not include the dilated filter construction. It increases the receptive field and learns the significant features for producing more effective solutions.

B. OWC-EDDNET

In EDDNet, each of the adapted networks is constructed by different layers to predict the fundamental data from the

given input. One advantage of using EDDNet is that DRNN provides better performance with exponentially increased dilation for the prediction model. DLSTM provides high accuracy in forecasting and the most precise prediction. DDBN model also achieves maximum accuracy rate and is used to classify features. At the same time, the models also have the drawbacks such as network skip connection, flexibility, and weight balance issues. To solve the limitations, the OWC-EDDNet is proposed, with the weight optimized by using developed EAOA. The output from each network is multiplied with weight to determine the average from all prediction scores and evaluate the final predicted outcome.

The final prediction with the optimal weight was determined using Eq. (36).

Final prediction

$$= w1 * ps1 + w2 * ps2 + w3 * ps3 + w4 * ps4 \quad (36)$$

Here $w1, w2, w3$ and $w4$ is the multiple predicted scores from RNN, LSTM, DBN, and DNN with weights. The weight ranges from $[0.01 - 0.99]$. $ps1, ps2, ps3$ and $ps4$ is the prediction score for RNN, LSTM, DBN, and DNN. The objective function of the developed OWC-EDDNetis explained in Eq. (37)

$$ObjFn = \arg \min_{\{w1, w2, w3, w4\}} [RMSE + MAE] \quad (37)$$

RMSE is the Root-Mean-Square error, MAE is the Mean Absolute Error respectively.

RMSE: It is the quadratic scoring rule, which measures the average magnitude error. The squared difference between the actual and prediction observation is shown in Eq. (38)

$$RMSE = \sqrt{\frac{\sum_{i=1}^e (n_i - m_i)^2}{p}} \quad (38)$$

MAE: It measures the average magnitude error in the prediction set. The Individual variations have equal weight as measured in Eq. (39)

$$MAE = \frac{\sum_{i=1}^e (n_i - m_i)}{p} \quad (39)$$

Here n and m is the observed and predicted value, p and e overall dimension, and fitted point. The average from all the prediction scores is determined, and the final predicted outcome is evaluated. The diagrammatic view of the proposed OWC-EDDNet is explained in Figure 3.

VI. RESULTS AND DISCUSSIONS

A. EXPERIMENTAL SETUP

The developed renewable power generation and consumption prediction framework was executed by employing the Python Paradigm, where the experimental estimation was done to show the proposed model’s effectiveness. The proposed model has 10 populations and included 4 chromosome lengths. Moreover, it has 50 highest iterations. The traditional models such as “CuttleFish Optimization (CFO)” [26], “Flow Direction Algorithm (FDA)” [27], “Garter Snake Optimization Algorithm (EGSOA) [28]” and “Artificial Orcas Algorithm (AOA) [25]” were utilized. Also the, classifiers like “RNN [20]”, “LSTM [18]”, “DBN [29]” and “EDDLNet [30]” were adopted.

B. PERFORMANCE MEASURES

MEP: “Mean error percentage” is to estimate the error by the variation of estimated and actual value is defined in Eq. (40)

$$MEP = \frac{100\%}{p} \sum_{i=1}^e \left(\frac{m_i - n_i}{m_i} \right) \quad (40)$$

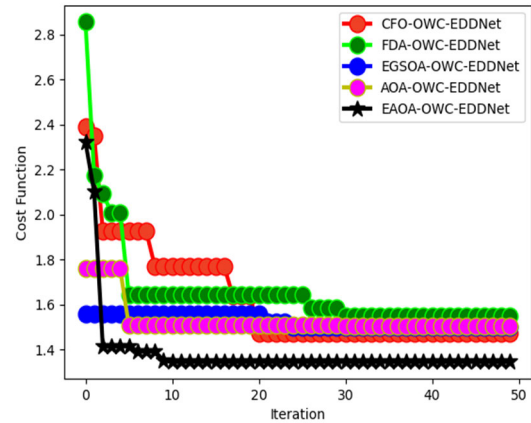


FIGURE 4. Cost function analysis of implemented power generation prediction model with optimized methods.

SMAPE: “Symmetric Mean Absolute Percentage Error” is to measure the accuracy according to the relative fault in Eq. (41)

$$SMAPE = \frac{100\%}{p} \sum_{i=1}^e \left(\frac{n_i - m_i}{n_i + m_i/2} \right) \quad (41)$$

MASE: “Mean Absolute Scaled Error” is to measure the average forecast correctness id formulated in Eq. (42)

$$MASE = \frac{1}{p} \sum_{i=1}^e \left(\frac{m_i - n_i}{m_i} \right) \quad (42)$$

One-Norm: It is the calculation of the total vector magnitude is shown in Eq. (43)

$$ON = \sum_i (K_i) \quad (43)$$

Two-Norm: It describes the optimal distance from one area to another computed in Eq. (44)

$$TN = \left(\sum_{i=1}^e K_i^2 \right)^{1/2} \quad (44)$$

Infinity-Norm: It is to calculate the vector length by using Eq. (45)

$$IN = \max_{1 \leq i \leq e} (K_i) \quad (45)$$

Here ‘K’ is the matrix value.

C. PERFORMANCE MEASURES

MEP: “Mean error percentage” is to estimate the error by the variation of estimated and actual value is defined in Eq. (46)

$$MEP = \frac{100\%}{p} \sum_{i=1}^e \left(\frac{m_i - n_i}{m_i} \right) \quad (46)$$

SMAPE: “Symmetric Mean Absolute Percentage Error” is to measure the accuracy according to the relative fault in

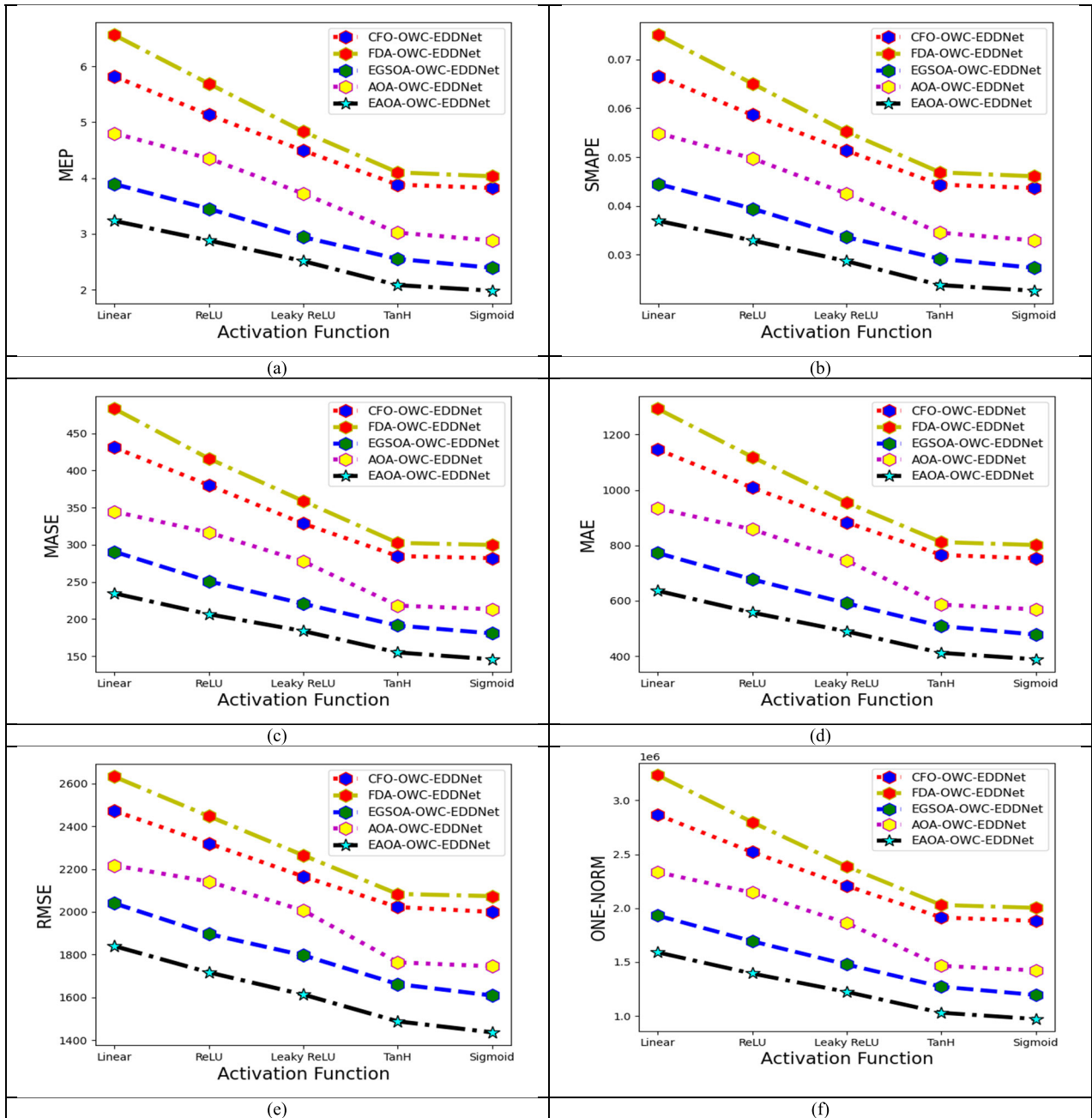


FIGURE 5. Performance evaluation of implemented power generation prediction model contrast with multiple existing algorithms regarding “(a) MEP, (b) SMAPE, (c) MASE, (d) MAE, (e) RMSE and (f) ONE-NORM.”

Eq. (47)

$$SMAPE = \frac{100\%}{p} \sum_{i=1}^e \left(\frac{n_i - m_i}{n_i + m_i/2} \right) \quad (47)$$

MASE: “Mean Absolute Scaled Error” is to measure the average forecast correctness id formulated in Eq. (48)

$$MASE = \frac{1}{p} \sum_{i=1}^e \left(\frac{m_i - n_i}{m_i} \right) \quad (48)$$

One-Norm: It is the calculation of the total vector magnitude

is shown in Eq. (49)

$$ON = \sum_i (K_i) \quad (49)$$

Two-Norm: It describes the optimal distance from one area to another computed in Eq. (50)

$$TN = \left(\sum_{i=1}^e K_i^2 \right)^{1/2} \quad (50)$$



FIGURE 6. Performance evaluation of implemented power generation prediction model contrast with multiple classifiers regarding “(a) MEP, (b) SMAPE, (c) MASE, (d) MAE, (e)RMSE and (f) ONE-NORM.”

Infinity-Norm: It is to calculate the vector length by using Eq. (51)

$$IN = \max_{1 \leq i \leq e} (K_i) \quad (51)$$

Here ‘K’ is the matrix value.

D. COST FUNCTION EVALUATION OF THE SUGGESTED FRAMEWORK OVER DIFFERENT OPTIMIZATION TECHNIQUES

The convergence determination of the designed method is accomplished, depicted in Figure 4. The cost function analysis estimates the PGP device. Various optimization models

TABLE 2. Comparative analysis of the developed power generation prediction model over distinct algorithms.

| TERMS | CFO-OWC-EDDNet [26] | FDA-OWC-EDDNet [27] | EGSOA-OWC-EDDNet [28] | AOA-OWC-EDDNet [25] | EAOA-OWC-EDDNet |
|-----------------|---------------------|---------------------|-----------------------|---------------------|-----------------|
| "MEP" | 3.88032305 | 4.100361297 | 2.550203 | 3.020258 | 2.080175 |
| "SMAPE" | 0.044347077 | 0.046861862 | 0.029146 | 0.034518 | 0.023774 |
| "MASE" | 284.7950882 | 302.5382839 | 191.2544 | 218.0368 | 154.9392 |
| "MAE" | 765.3624 | 811.7576 | 508.7056 | 586.0128 | 412.0708 |
| "RMSE" | 2022.221679 | 2083.678218 | 1662.479 | 1763.909 | 1488.266 |
| "ONE-NORM" | 1913406 | 2029394 | 1271764 | 1465032 | 1030177 |
| "TWO-NORM" | 101111.084 | 104183.9109 | 83123.96 | 88195.46 | 74413.28 |
| "INFINITY-NORM" | 7497 | 7451 | 7471 | 7479 | 7482 |

TABLE 3. Comparative analysis of the implemented power generation prediction framework over distinct classifiers.

| TERMS | RNN [4] | LSTM [2] | DBN [29] | EDDLNet [30] | EAOA-OWC-EDDNet |
|-----------------|-------------|-------------|----------|--------------|-----------------|
| "MEP" | 3.410296319 | 4.14035454 | 2.340173 | 2.840224 | 2.080175 |
| "SMAPE" | 0.038975299 | 0.047318917 | 0.026745 | 0.03246 | 0.023774 |
| "MASE" | 252.4853237 | 301.9258154 | 180.099 | 215.6728 | 154.9392 |
| "MAE" | 669.4584 | 816.9132 | 477.5756 | 570.3972 | 412.0708 |
| "RMSE" | 1893.210119 | 2090.699641 | 1621.085 | 1761.951 | 1488.266 |
| "ONE-NORM" | 1673646 | 2042283 | 1193939 | 1425993 | 1030177 |
| "TWO-NORM" | 94660.50596 | 104534.982 | 81054.26 | 88097.53 | 74413.28 |
| "INFINITY-NORM" | 7482 | 7449 | 7475 | 7482 | 7482 |

TABLE 4. Statistical evaluation of the developed power generation prediction model over distinct algorithm.

| TERMS | CFO-OWC-EDDNet [26] | FDA-OWC-EDDNet [27] | EGSOA-OWC-EDDNet [28] | AOA-OWC-EDDNet [25] | EAOA-OWC-EDDNet |
|--------|---------------------|---------------------|-----------------------|---------------------|-----------------|
| Worst | 2.392187093 | 2.855803012 | 1.559275 | 1.760806 | 2.323763 |
| Best | 1.474158567 | 1.550175741 | 1.500047 | 1.507339 | 1.346402 |
| Mean | 1.627925641 | 1.659951407 | 1.526369 | 1.53323 | 1.389542 |
| Median | 1.474158567 | 1.643032531 | 1.500047 | 1.508427 | 1.346402 |
| Std | 0.225454106 | 0.218888153 | 0.028554 | 0.07586 | 0.170721 |

differentiate the proposed system. In this, the cost function is varied with the amount of iterations. The iteration value starts from 0 to 50, whereas the measure of the cost function commences from 1.4 to 2.8. The cost factor of the suggested model is decreased by 82 % of CFO-OWC-EDDNet, 83.5 % of FDA-OWC-EDDNet, 84.2 % of EGSOA-OWC-EDDNet and 85 % of AOA-OWC-EDDNet appropriately for the 10th iteration. Thus, the findings explained that the designed framework has better management for cost.

E. PERFORMANCE ANALYSIS OF THE RECOMMENDED MODEL OVER DIFFERENT OPTIMIZATION MODELS

The performance estimation of the developed model over different optimization models is shown in Figure 5. Here, the functionality measures of the developed model are estimated with the activation function. The variable of the activation function varies as linear, ReLU, leaky ReLU, tanh and sigmoid. From Figure 5 (a), the MEP of the implemented model decreased by 5.3 % of CFO-OWC-EDDNet [26], 5.9 % of FDA-OWC-EDDNet [27], 3.8 % of EGSOA-OWC-EDDNet [28] and 4.5 % of AOA-OWC-EDDNet [25] respectively, when considering the activation function as ReLU. This confirms the suggested model has better performance than other models.

F. PERFORMANCE EVALUATION OF THE RECOMMENDED MODEL OVER DIFFERENT CLASSIFIERS METHODS

The performance analysis of the suggested method over different classifiers is shown in Figure 6. Here, the functionality

measures of the proposed method are calculated with the activation function. From Figure 6 (e) the RMSE of the recommended model is minimized by 24 % of RNN [4], 25 % of LSTM [2], 19 % of DBN [29] and 23% of EDDLNet [30], respectively, when considering the activation function as linear. This confirms the suggested model has better performance than other models.

G. PERFORMANCE EVALUATION OF THE RECOMMENDED MODEL OVER DIFFERENT CLASSIFIERS METHODS

The performance analysis of the suggested method over different classifiers is shown in Figure 6. Here, the functionality measures of the proposed method are calculated with the activation function. From Figure 6 (e) the RMSE of the recommended model is minimized by 24 % of RNN [4], 25 % of LSTM [2], 19 % of DBN [29] and 23% of EDDLNet [30], respectively, when considering the activation function as linear. This confirms the suggested model has better performance than other models.

H. COMPARATIVE ANALYSIS OF THE RECOMMENDED MODEL OVER VARIOUS OPTIMIZATION MODELS AND CLASSIFIERS.

Table 2 and Table 3 shows the comparative analysis of the implemented model over various optimization models and classifiers accordingly. From Table 2, the MAE of the developed model reduced by 85 % of CFO-OWC-EDDNet, 96 % of FDA-OWC-EDDNet, 23 % of EGSOA-OWC-EDDNet

and 42 % of AOA-OWC-EDDNet respectively. This confirms the suggested model has better efficiency than other models.

I. STATISTICAL ANALYSIS OF THE RECOMMENDED MODEL OVER VARIOUS OPTIMIZATION MODEL

The statistical evaluation of the recommended model is estimated over different optimization models shown in Table 4. The designed model raised by 9.4 % of CFO-OWC-EDDNet, 15.1 % of FDA-OWC-EDDNet, 11.4 % of EGSOA-OWC-EDDNet And 11.9% of AOA-OWC-EDDNet by taking the best measures. Hence the outcome shows the suggested model outperformed better than other existing models. 11.9% of AOA-OWC-EDDNet by taking the best measures. Hence the outcome shows the suggested model outperformed better than other existing models.

VII. CONCLUSION

The framework of renewable power generation forecasting with the developed EAOA model was implemented. At first, the power plant data were collected and then the data was pre-processed by data aggregation and scaling process. From the pre-processed data the features were extracted by higher-order statistical features. The output feature was given to OWC-EDDNet, where each network predicted the generated power and the weight-optimized by the developed EAOA for better prediction. Finally, the average of the prediction score was evaluated. The efficacy of the designed framework was analyzed by various performance factors and existing techniques. The MAE of the implemented model was decreased by 10.5 % of CFO-OWC-EDDNet, 11.5 % of FDA-OWC-EDDNet, 7 % of EGSOA-OWC-EDDNet and 9 % of AOA-OWC-EDDNet appropriately when considering the ReLU activation function. Thus the finding revealed the implemented system had higher efficiency than other traditional models.

REFERENCES

- [1] Y. He, Z. Huang, and B. Sick, "Toward application of continuous power forecasts in a regional flexibility market," in *Proc. Int. Joint Conf. Neural Netw. (IJCNN)*, Jul. 2021, pp. 1–8.
- [2] G. Marulanda, J. Cifuentes, A. Bello, and J. Reneses, "Short-term wind power forecasting by a long short term memory ensemble approach," in *Proc. 13th Int. Renew. Energy Congr. (IREC)*, Dec. 2022, pp. 1–6.
- [3] V. Muniyandi, S. Manimaran, P. R. Ramu, and S. Gangatharan, "A comprehensive analysis of recent advances in deep learning based solar irradiance forecasting," in *Proc. 7th Int. Conf. Trends Electron. Informat. (ICOEI)*, Apr. 2023, pp. 1250–1257.
- [4] B. Ray, R. Shah, M. R. Islam, and S. Islam, "A new data driven long-term solar yield analysis model of photovoltaic power plants," *IEEE Access*, vol. 8, pp. 136223–136233, 2020.
- [5] Q. Li, Y. Yu, T. Lin, X. Fu, H. Du, and X. Xu, "Deep reinforcement learning-based fast prediction of strategies for security control," in *Proc. IEEE 5th Conf. Energy Internet Energy Syst. Integr. (EI)*, Oct. 2021, pp. 2737–2742.
- [6] S. Liu, S. Han, and S. Zhu, "Reinforcement learning-based energy trading and management of regional interconnected microgrids," *IEEE Trans. Smart Grid*, vol. 14, no. 3, pp. 2047–2059, May 2023.
- [7] J. Jeong and H. Kim, "DeepComp: Deep reinforcement learning based renewable energy error compensable forecasting," *Appl. Energy*, vol. 294, Jul. 2021, Art. no. 116970.
- [8] U. Singh and M. Rizwan, "SCADA system dataset exploration and machine learning based forecast for wind turbines," *Results Eng.*, vol. 16, Dec. 2022, Art. no. 100640.
- [9] W. Cui, C. Wan, and Y. Song, "Ensemble deep learning-based non-crossing quantile regression for nonparametric probabilistic forecasting of wind power generation," *IEEE Trans. Power Syst.*, vol. 38, no. 4, pp. 3163–3178, 2022.
- [10] Y. Huang, J. Li, W. Hou, B. Zhang, Y. Zhang, Y. Li, and L. Sun, "Improved clustering and deep learning based short-term wind energy forecasting in large-scale wind farms," *J. Renew. Sustain. Energy*, vol. 12, no. 6, Nov. 2020.
- [11] Z. Ma, H. Chang, Z. Sun, F. Liu, W. Li, D. Zhao, and C. Chen, "Very short-term renewable energy power prediction using XGBoost optimized by TPE algorithm," in *Proc. 4th Int. Conf. HVDC (HVDC)*, Nov. 2020, pp. 1236–1241.
- [12] L. Li, G. Z. Qiang, X. Yao-Qiang, and Z. Dong-Hua, "Large-scale wind and solar grid-connected power prediction based on causal delay spectrum and LSTM," in *Proc. China Int. Conf. Electr. Distribution (CICED)*, Apr. 2021, pp. 76–80.
- [13] J. Rodway, P. Musilek, S. Misak, and L. Prokop, "Prediction of voltage related power quality values from a small renewable energy installation," in *Proc. IEEE Elect. Power Energy Conf.*, Nov. 2021, pp. 76–81.
- [14] O. Eyecioglu, B. Hangun, K. Kayisli, and M. Yesilbudak, "Performance comparison of different machine learning algorithms on the prediction of wind turbine power generation," in *Proc. 8th Int. Conf. Renew. Energy Res. Appl. (ICRERA)*, Nov. 2019, pp. 922–926.
- [15] Y. Xue, R. Li, X. Hua, and X. Feng, "Short-term photovoltaic power prediction of bi-LSTM based on MIC," in *Proc. 6th Int. Conf. Power Renew. Energy (ICPRE)*, Sep. 2021, pp. 1107–1111.
- [16] Z. YanQi, Z. Qiang, Z. Long, D. Kun, W. Dingmei, and Z. Ruixiao, "The key technology for optimal scheduling and control of wind-photovoltaic-storage multi-energy complementary system," in *Proc. IEEE Sustain. Power Energy Conf. (ISPEC)*, Nov. 2020, pp. 1517–1522.
- [17] Z. A. Khan, T. Hussain, and S. W. Baik, "Boosting energy harvesting via deep learning-based renewable power generation prediction," *J. King Saud Univ. Sci.*, vol. 34, no. 3, Apr. 2022, Art. no. 101815.
- [18] W. Khan, S. Walker, and W. Zeiler, "Improved solar photovoltaic energy generation forecast using deep learning-based ensemble stacking approach," *Energy*, vol. 240, Feb. 2022, Art. no. 122812.
- [19] Y.-Y. Hong and C. L. P. P. Rioflorida, "A hybrid deep learning-based neural network for 24-h ahead wind power forecasting," *Appl. Energy*, vol. 250, pp. 530–539, Sep. 2019.
- [20] N. Shabbir, L. Kut, M. Jawad, O. Husev, A. Ur Rehman, A. A. Gardezi, M. Shafiq, and J.-G. Choi, "Short-term wind energy forecasting using deep learning-based predictive analytics," *Dept. Elect. Power Eng. Mechatronics*, vol. 72, no. 1, pp. 1017–1033, 2022.
- [21] A. Alshammari, "Generation forecasting employing deep recurrent neural network with metaheuristic feature selection methodology for renewable energy power plants," *Sustain. Energy Technol. Assessments*, vol. 55, Feb. 2023, Art. no. 102968.
- [22] G. Wang, Q.-S. Jia, and D. Din, "Deep learning-based model predictive control for continuous stirred-tank reactor system," *Appl. Electron. Sci.*, vol. 32, 2022.
- [23] Z. Qian, S. Wen, L. Zhang, J. Zhang, S. Yuan, L. Mao, and L. Zhou, "Deep learning-based short-term wind power prediction considering various factors," in *Proc. 17th Int. Conf. Control, Autom., Robot. Vis. (ICARCV)*, Dec. 2022, pp. 529–533.
- [24] S. Thejus and P. Sivraj, "Deep learning-based power consumption and generation forecasting for demand side management," in *Proc. 2nd Int. Conf. Electron. Sustain. Commun. Syst. (ICESC)*, Aug. 2021, pp. 1350–1357.
- [25] H. Drias, L. S. Bendimerad, and Y. Drias, "A three-phase artificial orcas algorithm for continuous and discrete problems," *Int. J. Appl. Metaheuristic Comput.*, vol. 13, no. 1, pp. 1–20, Sep. 2022.
- [26] A. S. Eesa, A. M. A. Brifciani, and Z. Orman, "Cuttlefish algorithm—A novel bio-inspired optimization algorithm," *Int. J. Sci. Eng. Res.*, vol. 4, no. 9, pp. 1978–1986, 2013.
- [27] H. Karami, M. V. Anaraki, S. Farzin, and S. Mirjalili, "Flow direction algorithm (FDA): A novel optimization approach for solving optimization problems," *Comput. Ind. Eng.*, vol. 156, Jun. 2021, Art. no. 107224.
- [28] M. Naghdiani, M. Jahanshahi, and R. K. Matin, "A garter snake optimization algorithm for constrained optimization," *Tech. Rep.*, May 2023, vol. 1.
- [29] Y. Hua, J. Guo, and H. Zhao, "Deep belief networks and deep learning," in *Proc. Int. Conf. Intell. Comput. Internet Things*, 2015, pp. 1–4.

[30] V. Chandran, M. G. Sumithra, A. Karthick, T. George, M. Deivakani, B. Elakkiya, U. Subramaniam, and S. Manoharan, "Diagnosis of cervical cancer based on ensemble deep learning network using colposcopy images," *BioMed Res. Int.*, vol. 2021, pp. 1–15, May 2021.

[31] A. Mukherjee and P. Mitra, "Predicting cyclone landfall using mutual information and dilated recurrent neural network," *Environ. Data Sci.*, vol. 1, p. e18, Jul. 2022.

[32] G. Dudek, P. Pelka, and S. Smyl, "A hybrid residual dilated LSTM and exponential smoothing model for midterm electric load forecasting," *IEEE Trans. Neural Netw. Learn. Syst.*, vol. 33, no. 7, pp. 2879–2891, Jul. 2022.

[33] G. Altan, N. Allahverdi, and Y. Kutlu, "Diagnosis of coronary artery disease using deep belief networks," *Eur. J. Eng. Natural Sci.*, vol. 2, no. 1, pp. 29–36, Feb. 2017.

[34] Z. Arabasadi, R. Alizadehsani, M. Roshanzamir, H. Moosaei, and A. A. Yarifard, "Computer aided decision making for heart disease detection using hybrid neural network-genetic algorithm," *Comput. Methods Programs Biomed.*, vol. 141, pp. 19–26, Apr. 2017.

[35] N. V. Kurdkandi, M. G. Marangalu, S. Mohammadsalehian, H. Tarzarni, Y. P. Siwakoti, M. R. Islam, and K. M. Muttaqi, "A new six-level transformer-less grid-connected solar photovoltaic inverter with less leakage current," *IEEE Access*, vol. 10, pp. 63736–63753, 2022.

[36] M. G. Marangalu, N. V. Kurdkandi, and E. Babaei, "Single-source multi-level inverter based on flyback DC–DC converter," *IET Power Electron.*, vol. 14, no. 7, pp. 1237–1255, May 2021.

[37] M. G. Marangalu, S. H. Hosseini, N. V. Kurdkandi, and A. Khoshkbar-Sadigh, "A new five-level switched-capacitor-based transformer-less common-grounded grid-tied inverter," *IEEE J. Emerg. Sel. Topics Power Electron.*, 2022.

[38] S. K. Vankadara, S. Chatterjee, and P. K. Balachandran, "An accurate analytical modeling of solar photovoltaic system considering R_s and R_{sh} under partial shaded condition," *Int. J. Syst. Assurance Eng. Manage.*, vol. 13, no. 5, pp. 2472–2481, Oct. 2022.

[39] T. Selvaraj, R. Rengaraj, G. Venkatakrishnan, S. Soundararajan, K. Natarajan, P. Balachandran, P. David, and S. Selvarajan, "Environmental fault diagnosis of solar panels using solar thermal images in multiple convolutional neural networks," *Int. Trans. Electr. Energy Syst.*, vol. 2022, pp. 1–16, Sep. 2022.

[40] F. Yu and V. Koltun, "Multi-scale context aggregation by dilated convolutions," 2015, *arXiv:1511.07122*.



ZHIFENG CHE received the degree from the Department of Computer Science and Technology, Henan Normal University, in 2003. He is currently with Xinxiang Vocational and Technical College. His research interests include computer science and technology, optimization techniques, deep learning, and the Internet of Things.



A. AMIRTHASARAVANAN received the Ph.D. degree from Anna University, Chennai, Tamil Nadu, India, in 2018. He is currently working as an Assistant Professor with the Department of Computing Technologies, SRM Institute of Science and Technology, Chennai, Tamil Nadu, India. His research interests include information security, cloud computing, and the IoT.

MUNA AL-RAZGAN received the Ph.D. degree in information technology from George Mason University, Fairfax, VA, USA. She is currently an Associate Professor in software engineering with the College of Computer and Information Sciences, King Saud University, Riyadh, Saudi Arabia. Her research interests include data mining, machine learning, artificial intelligence, educational data mining, and assistive technologies.



EMAD MAHROUS AWWAD was born in Minya, Egypt, in 1988. He received the degree, in 2011, and the M.Sc. degree in electrical engineering from the Department of Electrical Engineering, King Saud University, in 2020, where he is currently pursuing the Ph.D. degree. He was a Teaching Assistant with the Department of Industrial Electronics and Control Engineering, Faculty of Electronic Engineering, Menofia University, Egypt, in 2012. His research interests include system design, control of linear and nonlinear systems, embedded system design, the Internet of Things (IoT), and implementation of autonomous mobile robots. He is also interested in modeling, optimization, observer design, model predictive controller of vehicle dynamics under the wheel-terrain interaction slippage phenomenon, artificial intelligence (AI), machine learning (ML), and deep learning (DL) related to the field of robotics and image processing.



MOHAMED YASIN NOOR MOHAMED received the M.C.A. degree from Bharathidasan University and the Ph.D. degree in computer science and engineering from Pondicherry University. He is currently a Senior Faculty Member of information technology with Sultan Qaboos University, Muscat, Oman. He has 23 years of a wide range of academic teaching skills and a strong research background. He has published one Australian patent, nine research articles in international peer-reviewed journals, and presented 12 research papers at international conferences. His research interests include wireless sensor networks, cloud computing, the Internet of Things, and embedded systems. He has visited various countries, such as France, Belgium, The Netherlands, Singapore, Malaysia, and USA for oral presentations at the international IEEE conferences.



VAIBHAV BHUSHAN TYAGI received the B.Tech. degree from Uttar Pradesh Technical University (UPTU), Lucknow, in 2007, the M.Tech. degree from IIT Roorkee, in 2011, and the Ph.D. degree, in 2015. He is currently an Associate Professor (ECE) and the Dean of FICT, ISBAT University, Kampala, Uganda. He has worked in several administrative and academic positions in India, Ethiopia, and Uganda. He has more than 13 years of research and teaching experience around the globe. His research interests include sensor applications in signal processing, signal modeling, artificial intelligence, and deep learning.